Biomedical Signal Processing and Control 87 (2024) 105560

Contents lists available at ScienceDirect

Biomedical Signal Processing and Control

journal homepage: www.elsevier.com/locate/bspc

A quantum convolutional network and ResNet (50)-based classification architecture for the MNIST medical dataset

Esraa Hassan [a], M. Shamim Hossain [b,*], Abeer Saber [c], Samir Elmougy [d], Ahmed Ghoneim [b], Ghulam Muhammad [e]

[a] Faculty of Artificial Intelligence, Kafrelsheikh University, Kafrelsheikh 33511, Egypt
[b] Research Chair of Pervasive and Mobile Computing, and Department of Software Engineering, College of Computer and Information Sciences, King Saud University, Riyadh 12372, Saudi Arabia
[c] Information Technology Department, Faculty of Computers and Artificial Intelligence, Damietta University, Damietta 34517, Egypt
[d] Dept. of Computer Science, Faculty of Computers and Information, Mansoura University, Mansoura 35516, Egypt
[e] Department of Computer Engineering, College of Computer and Information Sciences, King Saud University, Riyadh, Saudi Arabia

ARTICLE INFO

Keywords:
Quantum Convolutional Neural Network
ResNet (50)
Medical classification
Biomedical imaging
Medical MNIST

ABSTRACT

Biomedical image classification is crucial for both computer vision tasks and clinical care. The conventional method requires a significant amount of time and effort for extracting and selecting classification features. Deep Neural Networks (DNNs) and Quantum Convolutional Neural Networks (QCNN) are emerging techniques in machine learning that have demonstrated their efficacy for various classification tasks. Because of the complexity of their designs, the results of such models may also be challenging to interpret. In this paper, we propose an architecture called Medical Quantum Convolutional Neural Network (MQCNN), based on the QCNN model and a modified ResNet (50) pre-trained model, for enhancing the biomedical image classification in the MNIST medical dataset. During the training phase, the weights are updated using the Adam optimizer, while ResNet (50) is used to reduce the computational cost. MQCNN is compared to the QCNN model, the ResNet (50) pre-trained model, and some other related works on the Medical MNIST dataset. The results showed that MQCNN model achieves 99.6% accuracy, 99.7% precision, 99.6% recall, and 99.7% F1 score, and outperforms the ResNet (50) pre-trained model, the QCNN model, and the other compared related works.

1. Introduction

With the increasing availability of medical imaging data such as X-rays, MRIs, and CT scans, there is a growing need for accurate and efficient methods to diagnose and classify bio-medical images. Biommedical image classification has the potential to reduce the diagnosis time, and to enhance the overall performances. Deep Learning (DL) techniques are being used to tackle more complex medical image data in the field of bio-medical image classification [1–3]. DL algorithms have been applied in bio-medical image classification to extract features from medical images such as tumors, lesions, and abnormal tissue growth. These algorithms can learn from vast datasets and recognize patterns that the human eye may miss. As medical images become more complex, deep learning algorithms evolve to become more efficient and accurate in their classifications. The challenge of locating high-quality images for the model's training is one of the problems with medical MNIST [2,4,5]. Since many bio-medical images are not accessible to the public, researchers are forced to use pre-existing datasets or build their own.

With the ability to process vast amounts of bio-medical image data quickly and accurately, DL algorithms have the potential to revolutionize medical diagnosis, leading to earlier detection and more effective treatments for a range of medical conditions. The principles of quantum computing enable more efficient data processing than conventional methods. It uses a combination of classical and quantum components with fewer parameters and quicker training times [6]. Quantum Neural Network (QNN) uses quantization techniques to reduce the size and complexity of Neural Networks (NN) while maintaining accuracy. It has been used in several studies for bio-medical image classification tasks such as lung cancer detection segmentation, in which its architecture enhances the accuracy and speed of the overall image classification tasks [3,6-9]. QNN has been extensively used in medical image classification studies, such as lung cancer detection segmentation, where its unique

* Corresponding author.
E-mail address: mshossain@ksu.edu.sa (M.S. Hossain).

https://doi.org/10.1016/j.bspc.2023.105560
Received 7 May 2023; Received in revised form 5 July 2023; Accepted 30 September 2023
Available online 7 October 2023
1746-8094/

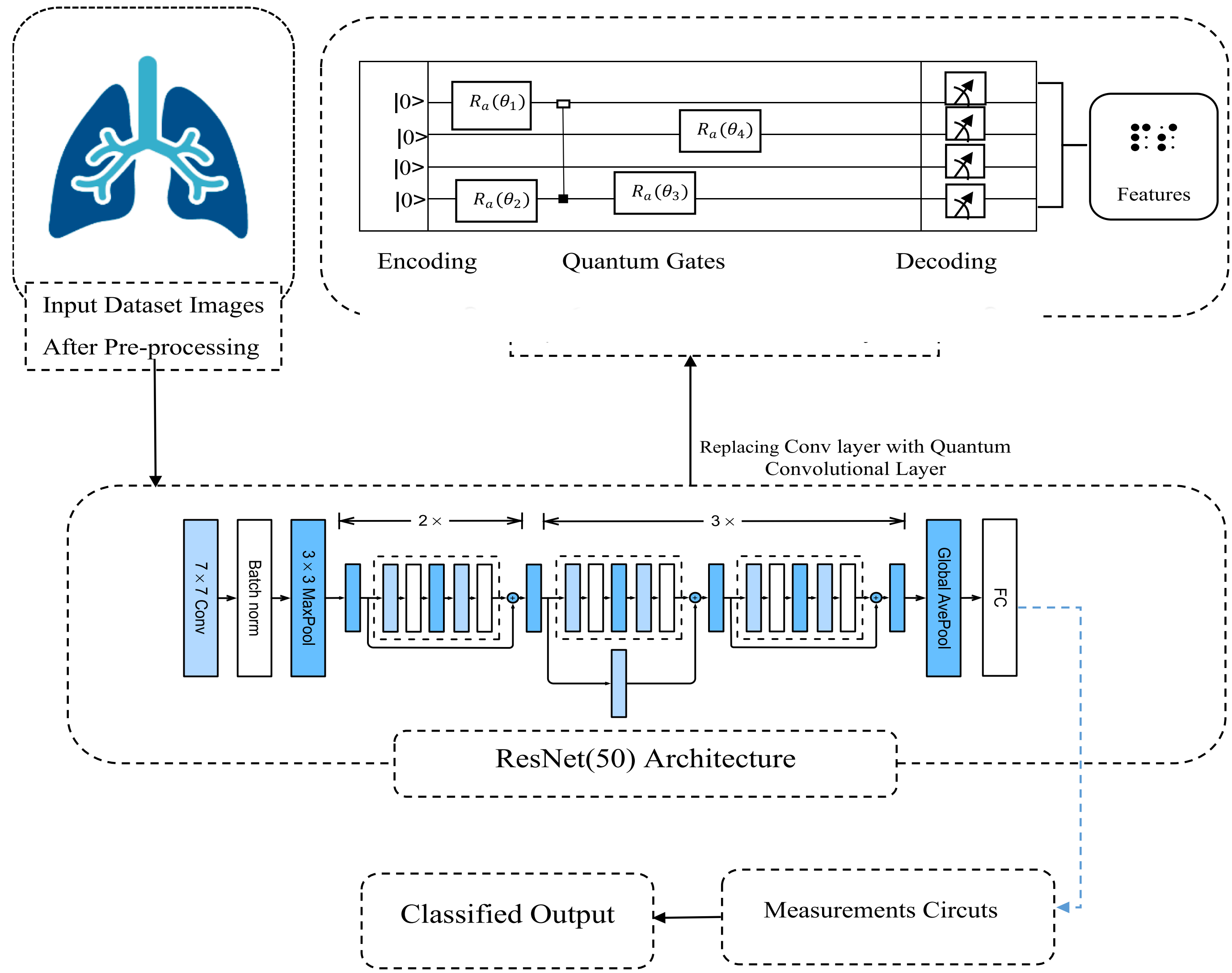

Fig. 1. The general architecture of the proposed MQCNN.

architecture enhances the accuracy and speed of image classification tasks. The ability of QNN to process vast amounts of data more efficiently than traditional DL methods has the potential to significantly improve the speed and accuracy of medical image analysis. With further advancements in QNN technology, it is likely that it will become an increasingly important tool in the field of bio-medical image classification, leading to more accurate diagnoses and better patient outcomes.

In this paper, we propose a Medical Quantum Convolutional Neural Network (MQCNN) model based on a modified ResNet (50) pre-trained model and QNN for the MNIST biomedical image dataset. MNIST dataset consists of 58,954 medical images divided into six classes [7–10]. This dataset is important because it enables scientists and programmers to build algorithms that can precisely identify medical disorders [9]. This can result in better patient outcomes and more accurate diagnoses. Moerover, this dataset can be used to train models for computer vision, image recognition and other related fields [10–12]. The proposed MQCNN architecture combines the QCNN model with a modified ResNet (50) pre-trained model. The QCNN model is based on quantum gates to manipulate input data and produce output from the measurement results. The ResNet (50) model combines Fully Connected Layers (FCLs), pooling layers, and convolutional layers to extract features from the images. The results of the conducted experimentation showed that the proposed work achieves better performance in classifying MNIST medical images. The contributions of this paper are summarized as follows:

- Proposing an MQCNN architecture based on a ResNet (50) pre-trained model and a quantum convolutional layer rather than employing ResNet (50) and Quantum Neural Network (QCNN) models separately to increase the performance of classifying the MNIST medical image dataset.
- Exploring the combination between the ResNet (50) pre-trained model and QCNN, where the quantum circuit applies a sequence of unitary operations to the input image, can be used to extract features that are difficult to capture with classical convolutional layers.
- Evaluating the proposed work and comparing its results with CNN model, QCNN model, and other related works in terms of accuracy, precision, recall, and F1-score metrics.

The remainder of the paper is structured as follows: The related work and background are illustrated in Section 2. The suggested work is presented in Section 3. Section 4 presents the experimentations and their results. The key points of this work are discussed in Section 5. The conclusion with some prospective future research topics are discussed in Section 6.

2. Background and related work

Biomedical imaging is an effective tool for visualizing interior organs of the body and an evidence-based medicine through explainable AI.

Table 1
The layers description in the proposed MQCNN architecture.

No.	Steps	Description
1	Input	Medical MINIST Dataset
2.	zero padding	It is used in the initial convolutional layer to preserve the spatial dimensions of the input image
Quanv	The threshold encoder	The threshold encoder is often used in QCNNs for error correction and fault-tolerance, as it allows the quantum information to be encoded into a classical format that can be easily manipulated and analyzed.
	Random Circuit	It is designed to explore quantum state space and enhance the learning capabilities of the QCNN.
	Measurement	Measurement QCNNs are a promising approach for quantum ML tasks, as they have the potential to outperform classical ML algorithms on certain types of data.
	Feature Maps	In QCNNs, the input quantum data is represented as a quantum state, and multiple layers of quantum gates are applied to the state to perform convolutional operations.
3	Batch Normalization	Batch normalization is used to stabilize the distribution of inputs to each layer, preventing the internal covariate shift problem where the distribution of inputs to a layer change during training, making it difficult for the network to learn effectively.
4	ReLU	It is applied after each convolutional layer in ResNet (50), including within the residual blocks. The ReLU activation function is defined as follows: $f(x) = \max(0, x)$
5	Max Pool	Max pooling is for downscaling the feature maps produced by convolutional layers and is a key component of many state-of-the-art DL architectures like ResNet (50).
6	Conv Block	The conv block is a key building block of the ResNet(50) architecture, used in the residual blocks to improve the accuracy and stability of the network. It consists of three convolutional layers, each followed by batch normalization and ReLU activation.
7	ID Block	The ID block is another building block used in the ResNet(50) architecture, used in the residual blocks when the input and output of the block have the same spatial dimensions. It consists of two convolutional layers, each followed by batch normalization and ReLU activation.
14	Avg pool	Average pooling works by dividing the feature map into non-overlapping rectangular regions (called pooling regions) and taking the average value within each region. The result is a down sampled feature map with reduced spatial dimensions and increased spatial invariance.
15	Flattening	Flattening works by taking the feature maps produced by the last convolutional layer or average pooling layer and reshaping them into a one-dimensional vector.
16	FC	The FC layer typically consists of more layers of densely connected neurons, where each neuron is connected to every neuron in the previous layer.
17	Output	The result is the one with the highest probability from (Abdomen CT, Head CT, BreastMRI, Chest CT, CXR, Hand).

Recently, applied AI, and explainable AI more specifically, deep learning, has dramatically impacted the field of Biomedical Imaging [13,14]. There has been a dramatic increase in research and development efforts focused on using AI in biomedical imaging for the purposes of precision medicine from its early and simple use of CXR in the diagnosis of fractures, biomedical imaging has evolved into a plethora of potent techniques used not only evidence-based medical care but also in the research of biological structure and function. In this section, we present QCNN background and the most recent related works for CT scan images depending on the medical MNIST dataset.

2.1. Background

2.1.1. Convolutional Neural Network (CNN)

To recognize and classify images, CNNs are particularly helpful because they can spot patterns in images that would be challenging for humans to notice. Its primary benefit is its capacity to learn from data without the need for manual feature engineering. However, one of the biggest issues with CNNs is their high processing demands, which can make it more challenging to implement them on mobile devices or other systems with limited resources. However, obtaining the quantity of labelled data that CNNs need to train efficiently can be challenging and time-consuming.

2.1.2. Quantum convolutional Neural Network (QCNN)

QCNN used the ideas of quantum computing and CNNs to process data more quickly and effectively than CNNs. It can also be able address the challenging issues that are beyond the capabilities of conventional computers. The fundamental issue with QCNNs is that they need specialized hardware and software to function, which can be expensive and challenging to design. The mathematical equation for the quantum convolution operation can be expressed as [15]:

$$|\psi\_out\rangle = U\_conv|\psi\_in\rangle \tag{1}$$

where $|\psi\_in\rangle$ represents the input quantum state, U_conv represents the quantum convolution gate, and $|\psi\_out\rangle$ represents the output quantum state.

2.1.3. ResNet(50) architecture

ResNet(50) is a Deep Neural Network (DNN) architecture that is commonly used for image classification tasks. Their architecture is designed to address the problem of vanishing gradients in DNNs using skip connections that allow the gradient to flow directly from the input to the output that consists of 50 layers and uses residual blocks to propagate information through the network. The mathematical equation for a residual block in ResNet(50) can be expressed as [16]:

$$y = F(x, \{Wi\}) + x \tag{2}$$

where x is the input to the block, y is the output of the block, F is a function that represents the convolutional layers with batch normalization and activation functions, and $\{Wi\}$ represents the parameters of the block.

2.2. Related works

Several studies for bio-medical computer vision tasks propose models to classify and segment many bio-medical datasets [12,17]. Anwar et al. [18] presented a deep CNN (DCNN) model for medical image classification that is robust to illumination changes. Their architecture contains 2 convolution layers, 2 max-pooling layers, and FCLs. The presented model is trained over a dataset of medical images with varying illumination conditions. The experimentations results showed that this work achieves superior results compared with the compared methods regards to the accuracy and robustness to illumination changes. Jiang et al. [19] presented a DL approach, called Deeply Supervised Layer Selective Attention Network (DSLSA-Net), for classifying medical

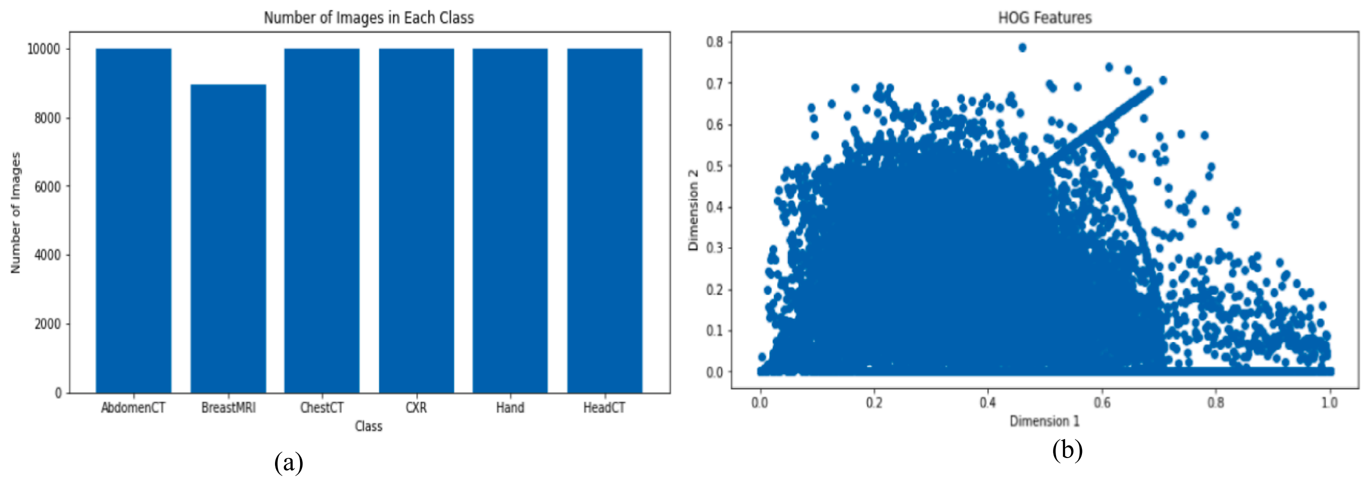

Fig. 2. (a) A bar diagram for the number of images in all classes. (b) The HOG features diagram.

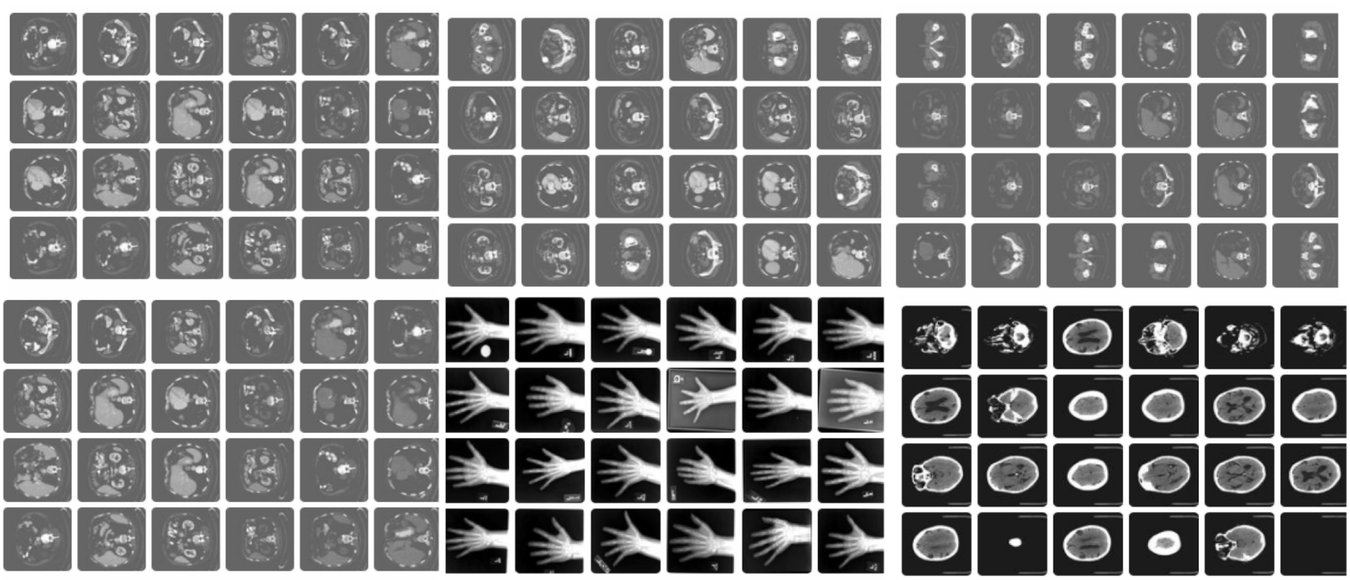

Fig. 3. Medical MINIST Dataset samples.

image to enhance the label-efficiency of learning by selectively attending to the most informative layers in DNN. The experimentations on two public datasets demonstrated that this work achieves superior performance compared to the compared methods, using fewer labels for training [17]. Zhang et al. [20] presented an approach for medical image analysis using Auto ML that combines the search on data augmentation and neural architecture, allowing for automated optimization of both components. The experimentations on several datasets demonstrated that this proposed work achieves superior performance compared to the compared methods.

Venkatesh et al. [21] presented a geometrical approach for detecting adversarial examples in batches. The proposed method uses a combination of geometric properties and statistical measures to detect adversarial examples. The authors showed that their method detects adversarial examples with high accuracy, even when the batch size is large. Also, they showed that this work is computationally efficient and can be used in real-time applications. Zheng et al. [22] presented an approach, called Implicit Distribution Representation (IDR), to label distribution learning. IDR is based on the idea that labels can be represented as a probability distribution over a latent space. This approach uses an implicit representation of the label distribution, which allows for more efficient learning and better generalization performance. Yang et al. [23] presented a large-scale lightweight benchmark (MedMNIST v2) to classify the 2D and 3D biomedical image. The used dataset is composed of a total of 10,000 images from 10 different classes, including 5 2D classes and 5 3D classes, and it provides a comprehensive evaluation of various DL models on different tasks, such as image classification and object detection. Additionally, it can be used to evaluate the performance of medical imaging modalities, such as CT scans and MRI scans. Rajaraman et al. [24] performed a systematic analysis of the effect of model calibration on its performance on chest X-rays and fundus images, based on VGG-16, Dense Net-121, Inception-V3, and EfficientNet-B0 classifiers and different variations including the imbalances degree in the training dataset, three calibration methods: Platt scaling, beta, and spline based on ECE metric, and both of classification default and optimal thresholds.

Valliani et al. [25] presented a general technique for ameliorating the effect of dataset shift using GANs. For classification, they used DenseNet architecture on chest radiographs to identify the opacities CXRs while used LeNet architecture for handwritten digits. Ragab et al. [26] proposed a diagnosis architecture for detecting Covid-19 for chest X-ray images based on dense convolutional and capsule NN (CapsNet)

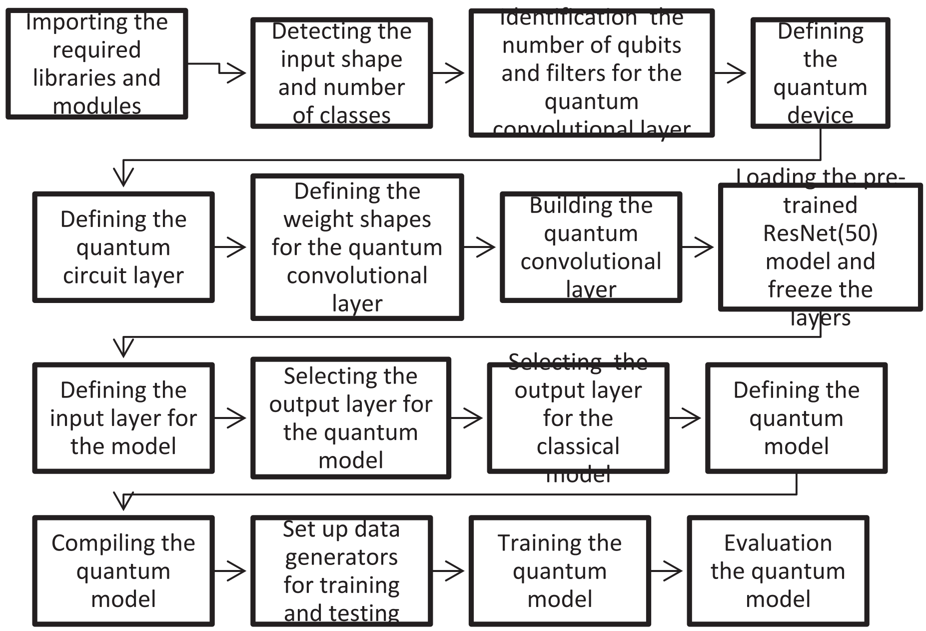

Fig. 4. The Main steps of the experiment MQCNN proposed model architecture.

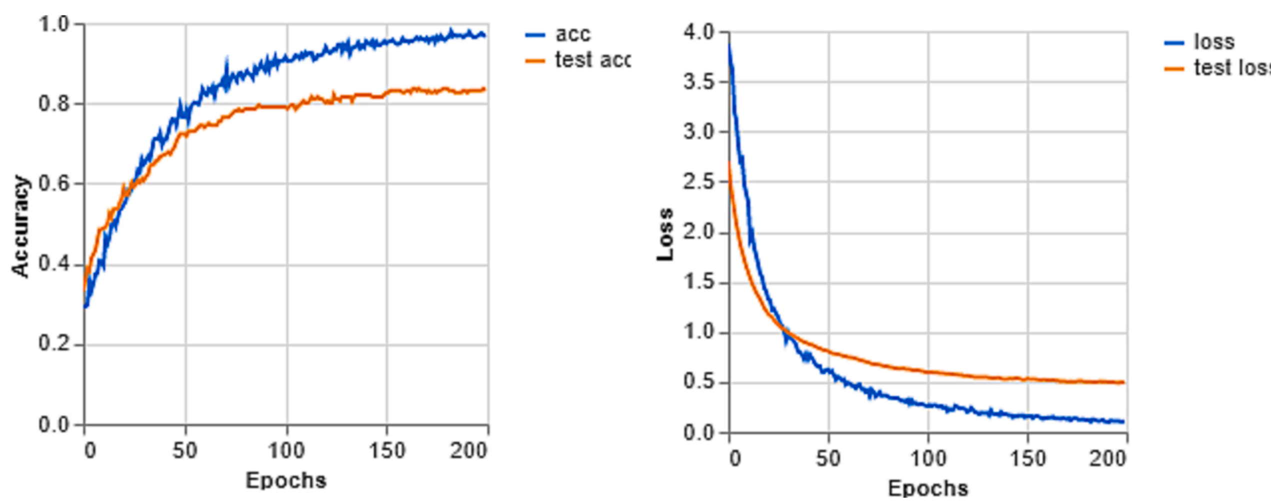

Fig. 5. The learning curves for QCNN architecture.

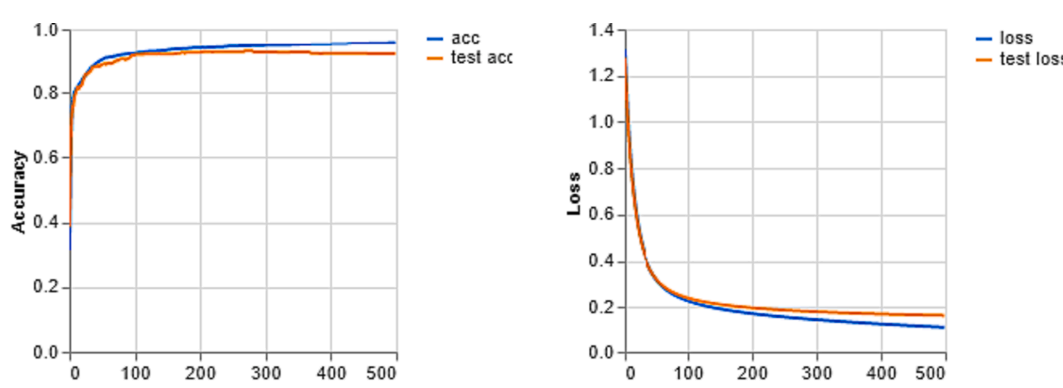

Fig. 6. The learning curves for ResNet (50) pre-trained model.

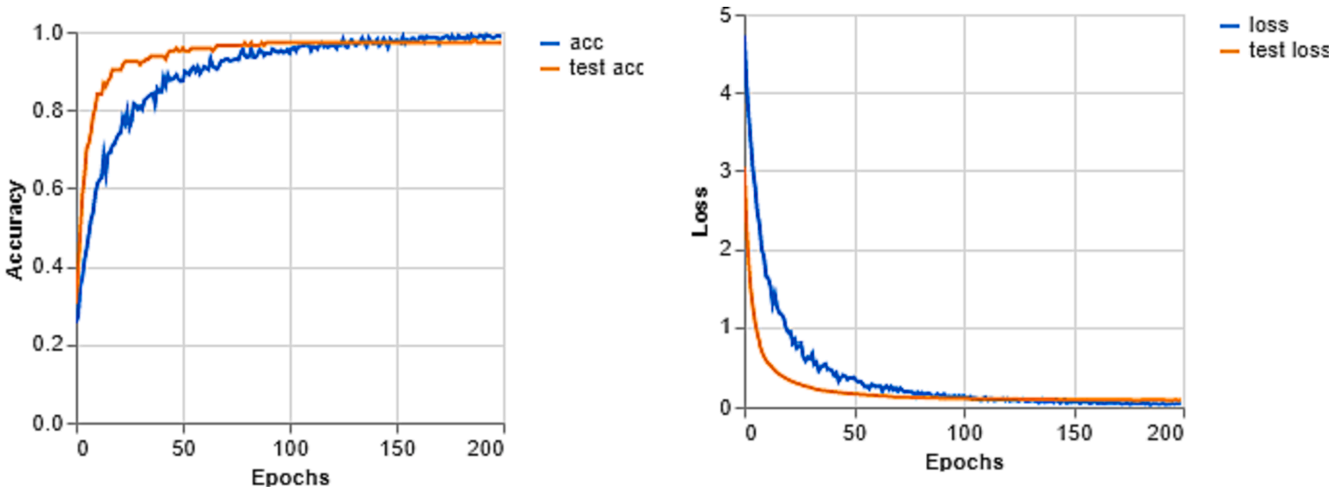

Fig. 7. The learning curves for MQCNN.

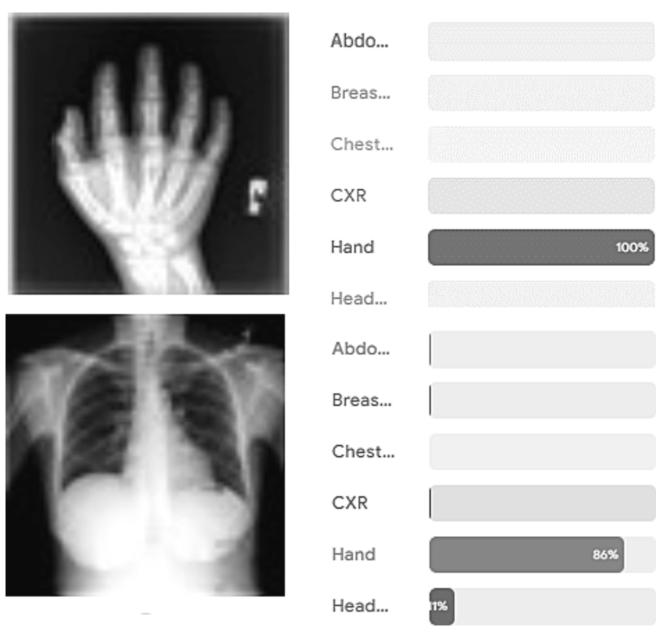

Fig. 8. Medical MINIST dataset visualization.

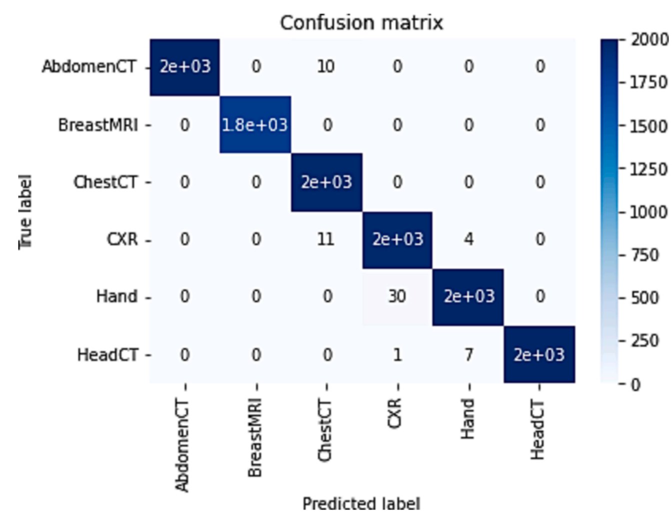

Fig. 9. Confusion matrix for MQCNN model.

models. Also, they applied dense convolutional model for classifying the images during the prediction process into normal, pneumonia, and COVID-19 categories; this proposed model achieved an accuracy of 95%. Nawaz et al. [27] proposed a deep learning, called CXray-EffDet, approach to detect chest abnormalities from NIH Chest X-ray images dataset. They presented a framework built on this approach to identify and categorize chest abnormality types. They applied employed EfficientNet-B0-based EfficientDet-D0 model for computing a distinctive set of sample key points. Awad et al. [28] presented a classification and image detection approach on X-ray and CT scan images. Their classification work used logistic regression while the detection used YOLOv4. To improve the accuracy of the classification, they used advanced parallel k-means pre-processing to identify the patterns and structures in the given data.

To increase the speed and the performance of the detection, they leveraged the acceleration ability of a neural engine processor. They showed that their work is efficient on different medical datasets. Li et al. [29] presented quantum–classical CNN model, HQCCNN, to classify images based on comprising quantum and classical components. The quantum convolutional layer, that has quantum convolution kernels built through parameterizing the quantum circuit, accomplishes the unitary transformation on the qubits related to the convolution window, while the quantum pooling is built from quantum pooling, accomplishes pooling operations. Stein et al. [30] proposed a quantum computing approach, QuCNN, from adapting CNN based on unbiased estimator. They used a test operation called SWAP on each trained filter to a get set of qubits. They exhibited an entanglement style back propagation of the training layers in NN to be predominantly on the quantum processor.

Ullah et al. [15] presented a quantum computing method as an adaptation of Fully CNN, FCQ-CNN. They used SVM with Recursive Feature Elimination to reduce the dimension in classifying ischemic heart diseases for IHD dataset, in which they showed that this work decreases the number of parameters and is an effective in training and testing of real quantum devices. Gupta et al. [31] employed DL and quantum machine learning (QML) techniques for diabetes prediction through utilizing a variational quantum circuit (QC) with tunning the hyperparameters and applying Adam optimizer to tune the parameters. QC is composed of three components: Encoder in which it encodes the input data into quantum states, the decoder that provides the output states, and the Evaluator that compares the output of the circuit with the related input labels. Li et al. [32] presented a Hybrid Quantum CNN model, HQCCNN, to classify images, that is consists of three layers: 1) Quantum Convolutional Layer (QCL), composed of some quantum convolution kernels that use quantum Parameterized Quantum Circuits (PQC) model for constructing, is used to operate as a linear unitary transformation on the given quantum state to obtain the feature map, 2) Quantum Pooling Layer (QPL) is used to reduce the convolution outputs and 3) The classical Fully Connected Layer (CFCL).

After evaluation of the quantum system, the identifiable quantum state (qubits) is measured, and the measurement outputs are fed to the classical fully connected layer to classify the image. A novel method for medical image analysis that has the potential to increase the precision and effectiveness of medical image classification tasks combines a Quantum Convolutional Network (QCN) with the ResNet-50 architecture. Further research is required to determine how the quantum convolutional layer affects the classification performance of the proposed approach in comparison to classical convolutional layers. Further study is necessary to comprehend the underlying biological mechanisms and support clinical decision-making, and the interpretability of the features learned by the quantum convolutional layer is a crucial factor in medical image analysis.

3. The proposed work

In this paper, we propose and develop an architecture, MQCNN, for classifying medical images based on QCNN model and a modified ResNet (50) pre-trained model. Recently, QCNN model has achieved robust performance in computer vision tasks, especially image classification. It is composed of the following stages: i) initializing the input data, ii) embedding input data into a quantum state, iii) using quantum gates to manipulate the quantum state, ix) measuring quantum gate output, and x) producing output from measurement results. In comparison to the effective pre-trained model, the ResNet (50) architecture has the following major stages: (i) preprocessing and preparing medical MNIST dataset for training; (ii) building the ResNet(50) model; (iii) training the model on medical MNIST dataset using Adam optimizer; (ix) evaluating the model's performance on the test set and adjusting hyperparameters if necessary to improve accuracy; and (x) deploying the model in a production environment and monitoring its performance over time.

The main difference between QCNN model and ResNet (50) architecture is the type of the used network [33,34]; QCNN classification uses QCNN while ResNet (50) classification uses a DCNN with 50 layers. CNN is designed to recognize patterns in images and classify them accordingly. QCNNs are more efficient than traditional CNNs, but they are still in the early stages of development and have not yet been widely adopted. Therefore, in this paper, we propose a MQCNN model based on a modified QCNN architecture that is used in the proposed study's training strategy to improve the performance.

In QCNN, a threshold encoder is a specific type of operation that is used to encode a quantum state into a classical bit string. The threshold encoder works by mapping the amplitudes of the input quantum state onto binary values, based on a threshold value. The threshold encoder takes as input a quantum state $|\psi\rangle$, with amplitudes a_i for each basis state $|i\rangle$. A random circuit is a type of quantum circuit where the gates applied to the qubits are selected randomly from a set of possible gates.

These circuits are interesting because they can be used to generate random quantum states and to study the properties of entanglement and coherence in quantum systems. In QCNN, the quantum states are processed through layers of quantum gates that are arranged in a grid-like pattern, with each gate acting on a small region of the quantum state. We can represent a random circuit as a sequence of randomly selected gates applied to the input state. Also, in QCNN, the feature maps are the quantum states resulting from applying a quantum filter to the input data. Mathematically, the operation of a quantum filter on the input data can be described by a quantum circuit that acts on a tensor product of the input data and a set of filter parameters. The output of this circuit is a quantum state, which can be represented as a density matrix. The feature map is then obtained by taking the trace of the density matrix with respect to the input data.

As shown in Fig. 1, the proposed MQCNN architecture is composed of three main steps: i) Pre-Processing: Performing pre-processing steps such as normalization, scaling, feature extracting, and dividing the dataset into 80–20% for training and testing, respectively. ii) Model Building: Building QCNN model using the training set of Medical MNIST dataset, training the model using an appropriate optimization algorithm such as gradient descent or Adam optimization, and evaluating the model on the test set to measure its performance. iii) Evaluation: Evaluate the performance of the QCNN model on the test set using metrics (accuracy, precision, recall, and F1 score), and compare the performance of QCNN model and ResNet (50) pre-trained model. Table 1 describes the layers in the proposed MQCNN architecture.

4. Experimental and results

In this section, we evaluate an architecture called MQCNN, which is based on the QCNN model and a modified ResNet (50) pre-trained model, for enhancing the biomedical image classification for Medical MNIST dataset. During the training stage, the weights are updated using the Adam optimizer, while ResNet (50) is used to reduce computational cost [2 35].

4.1. Dataset

Medical MNIST, also known as the MedNIST dataset for radiology and medical imaging in 64x64 dimensions for the preprocessing step, consists of 58,954 medical images divided into six classes [2], such as abdominal CT, head CT, breast MRI, chest CT, CXR, and Hand classes. The AbdomenCT class contains 10,000 images from Computed Tomography (CT) to diagnose and monitor conditions affecting the organs in the abdominal area. Head CT class contains 8954 images from CT scans of the head to diagnose and monitor conditions affecting the brain. BreastMRI contains 10,000 images from Magnetic Resonance Imaging (MRI) scans of the breast to diagnose and monitor breast cancer and other breast conditions. The chest CT class contains 10,000 images from CT scans of the chest to diagnose and monitor conditions affecting the lungs, such as pneumonia, lung cancer, and pulmonary embolism [17]. The CXR class contains 10,000 images from chest X-rays to diagnose and monitor conditions affecting the lungs and chest, such as pneumonia, tuberculosis, and lung cancer. The Hand class contains 10,000 images from X-rays of the hand used to diagnose and monitor conditions affecting the hand's bones and joints. Fig. 2 illustrates a bar diagram for the number of images in all classes that are considered a balanced dataset and shows the HOG features that can be used to capture the characteristic features of medical scans that are indicative of different medical conditions. By using HOG features as input to a proposed model, the model can learn to recognize these patterns and accurately classify medical scans into six categories. Fig. 3 shows a sample of this dataset.

4.2. Training and evaluation

The MNIST medical dataset is first preprocessed to ensure that it is in the appropriate format for the model, such as resizing the images, converting them to grayscale, and normalising the pixel values. The dataset is then split into training, validation, and test sets, using 80–20% for training and testing, respectively. For QCN, we use a batch size of 32, which means that the model is trained on 32 images at a time. For

Table 2
The comparison results between the proposed QCNN, ResNet(50), and QCNN architecture.

The Performance Measures				
Sensitivity	Specificity	Precision	Negative Predictive Value	False Positive Rate
TPR = TP / (TP + FN)	SPC = TN / (FP + TN)	PPV = TP / (TP + FP)	NPV = TN / (TN + FN)	FPR = FP / (FP + TN)
QCNN Architecture				
0.9836	0.9722	0.9677	0.9859	0.0278
ResNet(50) Architecture				
0.9836	0.9887	0.9868	0.9859	0.0113
The Proposed MQCNN Architecture				
0.9934	0.9887	0.9868	0.9943	0.0113

ResNet (50), we use a batch size of 64. In this section, the training and evaluation steps of the MQCNN proposed architecture, that depend on the QCNN and ResNet (50) architectures, are presented. Fig. 4 illustrates the main steps of implementation, where the first step is to determine the shape of the input data and the number of classes in the dataset for identifying the number of qubits and filters for the quantum convolutional layer are identified. A quantum circuit layer is defined to perform quantum convolutional operation. The weight shapes for the quantum convolutional layer are defined based on the number of qubits and filters. The pre-trained ResNet (50) model is loaded, and its layers are frozen to avoid overfitting. The output layer for the quantum model is selected, which is the quantum convolutional layer. The quantum model is compiled with the Adam optimizer and a categorical cross-entropy loss function; Adam optimizer is a popular optimization algorithm used for stochastic gradient descent. The learning process for a quantum image classification problem involves preparing a training set of quantum images. In this approach, the probability distribution of the output is obtained by performing a quantum measurement on the qubits that represent the label information. To optimize the MQCNN that is used for this task, the loss function is defined as the cross-entropy loss between the predicted probability distribution of the output and the ground truth label of the input image. The loss function is described as [36]:

$$L\left(f\left(I^{(i)},\Omega\right),y^{(i)}\right) = -\sum_{j=0}^{k-1}\left({y_j}^{(i)}*log{\overline{y}_j}^{(i)}\right) \tag{3}$$

where Ω denotes the parameters of QDCNN which is needed to be optimized. Obviously, ${\overline{y}_j}^{(i)}$ is the probability of the j-th quantum basis state. The updating of the parameters is carried out using Adam algorithm to update the values of the parameters in Ω iteratively during the training process, with the goal of minimizing the loss function.

Schrödinger's Equation (4) offers an accurate description of the behavior of quantum systems, so this equation is used in MQCNNs to improve the architecture. However, solving this equation for certain systems can be challenging, particularly those with multiple particles or intricate interactions. We use Schrödinger equation, which describes the behaviour of particles on a quantum level, to calculate the wavefunction of a particle, which can then be used to determine its properties such as energy, momentum, and position and is given as [30]:

$$i\hbar\partial\Psi(x,t)/\partial t = H\Psi(x,t) \tag{4}$$

where Ψ (x, t) is the wave function of the system, H is the Hamiltonian operator, i is the imaginary unit, t is time, and $\hbar$ is the reduced Planck constant.

ResNet (50) achieved the satisfied results when applied to medical MNIST dataset images. Fig. 5 and Fig. 6 show the learning curves for QCNN and ResNet(50), respectively, while Fig. 7 shows the learning curves for MQCNN. MQCNN achieved robust results when applied to medical MNIST dataset images. Some visualization for a medical MNIST dataset is shown in Fig. 8. Some metrics are computed based on the constructed confusion matrix, shown in Fig. 9, to evaluate the performance of the proposed model and identifies areas where further improvements can be made. The MQCNN architecture model performs with high accuracy for each class. Most instances are classified correctly, with very few misclassifications. However, there are some misclassifications in the CXR and Hand classes, where a few instances were classified as a different class. This information can be used to improve the model's performance by focusing on these classes during training or by tuning the model's hyperparameters.

4.3. Discussion

QCNN classification architecture is a form of CNN designed particularly for classifying medical images. It contains multiple convolutional layers, pooling layers, and FCLs that are trained using supervised learning techniques. The architecture is designed for extracting features from the input and classifying them into different categories. Using both of QCNN and Res-Net50 for Medical MNIST can help in improving the accuracy and speed of medical image classification tasks. By using this architecture, researchers can quickly train models on large datasets with high accuracy results. Additionally, this architecture can extract features from the input images more effectively than traditional CNNs, resulting in better performance on the medical image classification tasks. To evaluate the performance of ResNet (50), QCNN, and the proposed QCNN on MNIST dataset, we trained them for 200 epochs with a batch size of 32 and used Adam optimizer with a learning rate of 0.000001.

The performance of both models is evaluated based on different metrics. Additionally, these models can extract more meaningful features from the input images than the traditional CNNs; this help in improving the performance on unseen data points as well as reducing the bias in the results due to the data imbalance or other factors presented in the medical datasets. The experiment is conducted using two different implementations of CNNs: one using traditional methods and the other using quantum computing techniques. The results demonstrate that MQCNN outperforms CNN for image classification tasks when using quantum computing techniques for data processing instead of using classical methods such as matrix multiplication or convolution operations that are used in traditional CNNs implementations. Thus, quantum computing could be used to enhance the performance and efficiency of DL networks where large datasets are involved, and complex operations are needed to be performed quickly and accurately. The comparison results between the proposed QCNN, ResNet(50), and QCNN is illustrated in Table. 2. The comparison with other related works also highlights the superior performance of the proposed MQCNN architecture.

The Performance Measures

False Discovery Rate	False Negative Rate	Accuracy	F1 Score	Matthews Correlation Coefficient
FDR = FP / (FP + TP)	FNR = FN / (FN + TP)	ACC = (TP + TN) / (P + N)	F1 = 2TP / (2TP + FP + FN)	$MCC = TP*TN - FP*FN / sqrt((TP + FP)*(TP + FN)*(TN + FP)*(TN + FN))$
QCNN Architecture				
0.0323	0.0164	0.9774	0.9756	0.9547
ResNet(50) Architecture				
0.0132	0.0164	0.9863	0.9852	0.9725
The Proposed MQCNN Architecture				
0.0132	0.0066	0.9909	0.9901	0.9816

5. Conclusion and future works

In this paper, we propose MQCNN architecture for classifying medical images in MNIST dataset based on QCNN model and modified ResNet (50) architecture. MQCNN achieved 99.6% accuracy, 99.7% precision, 99.6% recall, and 99.7% F1 score, whereas ResNet (50) pretrained model achieved 98.9% accuracy, 98.9% precision, 98.9% recall, and 98.9% F1 score, and QCNN classification achieved 97.5% accuracy. In addition, the experimental results demonstrated that the proposed MQCNN architecture outperforms the other compared works. In our forthcoming study, we plan to investigate and implement additional architectures and methodologies in an attempt to improve the performance of bio-medical image classification. We also plan to investigate how various pre-processing techniques affect the performance of these models on the Medical MINIST dataset.

CRediT authorship contribution statement

Esraa Hassan: Conceptualization, Methodology. **M. Shamim Hossain:** Conceptualization, Funding acquisition, Supervision, Writing – review & editing. **Abeer Saber:** Methodology, Validation, Data curation. **Samir Elmougy:** Methodology, Validation, Project administration. **Ahmed Ghoneim:** Visualization, Project Administration. **Ghulam Muhammad:** Conceptualization, Validation.

Declaration of Competing Interest

The authors declare that they have no known competing financial interests or personal relationships that could have appeared to influence the work reported in this paper.

Data availability

Data will be made available on request.

Acknowledgements

The authors extend their appreciation to the Deputyship for Research & Innovation, Ministry of Education in Saudi Arabia for funding this research (IFKSURC-1-0304)

References

[1] W. Senior, et al., Improved protein structure prediction using potentials from deep learning, Nature 577 (7792) (2020) 706–710, https://doi.org/10.1038/s41586-019-1923-7.
[2] Dataset Availability at: https://www.kaggle.com/datasets/andrewmvd/medical-mnist.
[3] E. Hassan, M.Y. Shams, N.A. Hikal, S. Elmougy, A novel convolutional neural network model for malaria cell images classification, Comput. Mater. Continua 72 (3) (2022) 5889–5907, https://doi.org/10.32604/cmc.2022.025629.
[4] J. Landman, et al., Quantum methods for neural networks and application to medical image classification, Quantum 6 (2022) 881.
[5] Y. Yang, S. Soatto, FDA: Fourier domain adaptation for semantic segmentation.
[6] M. Nakajima, et al., Neural schrödinger equation: Physical law as deep neural network, IEEE Trans. Neural Networks Learn. Syst. 33 (6) (2021) 2686–2700.
[7] Z. Xu, et al., ISANET: Non-small cell lung cancer classification and detection based on CNN and attention mechanism, Biomed. Signal Process. Control 77 (2022), 103773.
[8] Q. Tian, A new optimized sequential method for lung tumor diagnosis based on deep learning and converged search and rescue algorithm, Biomed. Signal Process. Control 68 (2021), 102761.
[9] M. Henderson, S. Shakya, S. Pradhan, T. Cook, Quanvolutional neural networks: powering image recognition with quantum circuits, Quantum Mach Intell 2 (1) (2020) 2, https://doi.org/10.1007/s42484-020-00012-y.
[10] M.S. Hossain, G. Muhammad, N. Guizani, Explainable AI and mass surveillance system-based healthcare framework to combat COVID-I9 like pandemics, IEEE Netw. 34 (4) (2020) 126–132.
[11] F.J. Duarte, T.S. Taylor, J.C. Slaten, On the probability amplitude of quantum entanglement and the Pauli matrices, Opt Quantum Electron, vol. 52, no. 2, Feb. 2020, doi: 10.1007/s11082-020-2205-1.
[12] S. Elmuogy, et al., An efficient technique for CT scan images classification of COVID-19, J. Intell. Fuzzy Syst. 40 (3) (2021) 5225–5238.
[13] Y. Wu, et al., A deep learning fusion model with evidence-based confidence level analysis for differentiation of malignant and benign breast tumors using dynamic contrast enhanced MRI, Bio. Signal Processing and Control 72 (2022), 103319.
[14] N. Sharma et al., A smart ontology based IoT framework for remote patient monitoring, in Biomedical Signal Processing and Control, vol. 68, 2021, 102717.
[15] U. Ullah, A.G.O. Jurado, I.D. Gonzalez, B. Garcia-Zapirain, A fully connected quantum convolutional neural network for classifying ischemic cardiopathy, IEEE Access 10 (2022) 134592–134605, https://doi.org/10.1109/ACCESS.2022.3232307.
[16] E. Hassan, et al., Enhanced deep learning model for classification of retinal optical coherence tomography images, Sensors 23 (12) (2023) 5393, https://doi.org/10.3390/s23125393.
[17] S. Minaee, R. Kafieh, M. Sonka, S. Yazdani, and G. Jamalipour, Medical Image Analysis, pp. 1–9, 2021.
[18] S.M. Anwar, M. Majid, A. Qayyum, M. Awais, M. Alnowami, M. Khan, Medical image analysis using convolutional neural networks: a review, J. Med. Syst., vol. 42, no. 11. Springer New York LLC, Nov 01, 2018.
[19] P. Jiang, J. Liu, L. Wang, Z. Ynag, H. Dong, J. Feng, Deeply supervised layer selective attention network: towards label-efficient learning for medical image classification, Sep. 2022, [Online]. Available: http://arxiv.org/abs/2209.13844.
[20] J. Zhang, D. Li, L. Wang, L. Zhang, Auto machine learning for medical image analysis by unifying the search on data augmentation and neural architecture, Jul. 2022, [Online]. Available: http://arxiv.org/abs/2207.10351.
[21] D.K. Venkatesh, P. Steinbach, Detecting Adversarial Examples in Batches – a geometrical approach, Jun. 2022, [Online]. Available: http://arxiv.org/abs/2206.08738.
[22] Z. Zheng, X. Jia, Label distribution learning via implicit distribution representation, Sep. 2022, [Online]. Available: http://arxiv.org/abs/2209.13824.
[23] J. Yang, R. Shi, D. Wei, et al., MedMNIST v2 - A large-scale lightweight benchmark for 2D and 3D biomedical image classification, Sci Data 10 (2023) 41, https://doi.org/10.1038/s41597-022-01721-8.
[24] S. Rajaraman, et al., Deep learning model calibration for improving performance in class-imbalanced medical image classification tasks, PLoS One 17 (1) (2022) e0262838.
[25] A.A. Valliani, et al., Deploying deep learning models on unseen medical imaging using adversarial domain adaptation, PLoS One 17 (10) (2022) e0273262.
[26] M. Ragab, et al, Multiclass classification of chest X-Ray images for the prediction of COVID-19 using capsule network, Computat. Intelligence Neurosci., vol. 2022, Article ID 6185013, 8 pages, 2022. https://doi.org/10.1155/2022/6185013.
[27] M. Nawaz, et al., Chest disease detection and classification from X-ray images using the EfficientDet model, Diagnostics 13 (2023) 248, https://doi.org/10.3390/diagnostics13020248.
[28] F.H. Awad, M.M. Hamad, L. Alzubaidi, Robust classification and detection of big medical data using advanced parallel K-Means clustering, YOLOv4, and logistic regression, Life 13 (2023) 691, https://doi.org/10.3390/life13030691.
[29] J. Yang, et al., MedMNIST v2 - A large-scale lightweight benchmark for 2D and 3D biomedical image classification, Sci. Data 10 (2023) 41, https://doi.org/10.1038/s41597-022-01721-8.

[30] Y. Stein, Y. Mao, J. Ang, A. Li, QuCNN: A Quantum Convolutional Neural Network with Entanglement Based Backpropagation, in: IEEE/ACM 7th Symposium on Edge Computing (SEC), Seattle, WA, USA, 2022, pp. 368–374, https://doi.org/10.1109/SEC54971.2022.00054.
[31] H. Gupta, H. Varshney, T.K. Sharma, et al., Comparative performance analysis of quantum machine learning with deep learning for diabetes prediction, Complex Intell. Syst. 8 (2022) 3073–3087, https://doi.org/10.1007/s40747-021-00398-7.
[32] W. Li, P.-C. Chu, G.-Z. Liu, Y.-B. Tian, T.-H. Qiu, S.-M. Wang, An image classification algorithm based on hybrid quantum classical convolutional neural network, Quantum Eng. (2022).
[33] S. Hitawala, Y. Li, X. Wang, D. Yang, Image Super-Resolution Using VDSR-ResNeXt and SRCGAN, Oct. 2018, [Online]. Available: http://arxiv.org/abs/1810.05731.
[34] L. Ouyang, Y. Ma, J.-H. Byun, An integrative loss function approach to multi-response optimization, Qual. Reliab. Eng. Int. 31 (2) (2015) 193–204.
[35] E. Hassan, M.Y. Shams, N.A. Hikal, S. Elmougy, The effect of choosing optimizer algorithms to improve computer vision tasks: a comparative study, Multimed Tools Appl. (Sep. 2022), https://doi.org/10.1007/s11042-022-13820-0.
[36] YaoChong Li, et al., A quantum deep convolutional neural network for image recognition, Quantum Sci. Technol. 5 (4) (2020), 044003.